

Cite as: Wang BM, DAI C, MA DC, et al. CT manifestations and clinical characteristics of pulmonary invasive mucinous adenocarcinoma [J]. Clin J Clin Res, 2024, 37(1): 52-56.

DOI: 10.13429/j.cnki.cjcr.2024.01.011

CT manifestations and clinical characteristics of pulmonary invasive mucinous adenocarcinoma

WANG Baoming, DAI Chen, MA Dongchun

Department of Thoracic Surgery, Anhui Chest Hospital, Hefei, Anhui 230000, China

Corresponding author: MA Dongchun, E-mail: 1275167441@qq.com

Abstract: Objective To investigate the CT imaging manifestations and clinicopathologic features of patients with primary pulmonary invasive mucinous adenocarcinoma (PIMA) diagnosed pathologically after surgery. **Methods** The clinical data of 78 patients with PIMA diagnosed pathologically after surgery in the Department of Thoracic Surgery of Anhui Chest Hospital from November 2019 to November 2021 were retrospectively analyzed. **Results** Among the 78 cases, 33 (42.3%) were male and 45 (57.7%) were female, aged (60.3±7.8) years in total, and serum carcinoembryonic antigen (CEA) was increased (>5 μg/L) in 9 cases (11.5%). According to the clinical characteristics, patients could be divided into the asymptomatic group (60 cases, 76.9%) and the symptomatic group (18 cases, 23.1%). The symptomatic group included 8 cases with coughing and coughing up mucus sputum, 4 cases with chest tightness and chest and back pain, and 6 cases with other symptoms. Imaging manifestations showed that 51 (65.4%) lesions were located in the inferior lobes of both lungs and 71 (91.0%) in the peripulmonary, of which 46 patients (59.0%) had completely solid pulmonary nodules, and common signs included shallow lobulation and short burrs. Postoperative pathologic stages I, II, IIIa were found in 61 (78.2%), 9 (11.5%) and 8 (10.3%) patients, respectively. Moreover, genetic testing was performed in 13 patients, of which 8 cases were detected with mutations of Kirsten rat sarcoma viral (KRAS) oncogene, and 1 case was detected with mutations of epidermal growth factor receptor (EGFR) gene. Twenty-two patients were tested for the expression of programmed death-ligand 1 (PD-L1), and totally 18 (81.8%) of these patients had a tumor proportional score (TPS) of <1%. **Conclusion** Except for expectoration of mucous sputum, PIMA has no specific clinical symptoms. CT manifestations show that the lesions usually occur in the inferior lobes and peripulmonary of the lungs, and most pulmonary nodules are completely solid, which with signs of shallow lobulation and short burrs. Laboratory tests show that the expression level of PD-L1 is low, and the mutations of the KRAS gene are relatively more frequent. These features have some value in the diagnosis and differential diagnosis of PIMA.

Keywords: Pulmonary mucinous adenocarcinoma; Inferior lobe of lung; Peripulmonary; Solid pulmonary nodules; Signs of shallow lobulation; Signs of short burrs; Programmed death-ligand 1; Kirsten rat sarcoma viral oncogene

Pulmonary invasive mucinous adenocarcinoma (PIMA) is a variant of lung adenocarcinoma. The prevalence of PIMA is lower than that of invasive non-mucinous adenocarcinoma, accounting for about 2%-5% of lung adenocarcinoma, and can coexist with non-mucinous adenocarcinoma. For mucinous adenocarcinoma components greater than 10%, it can be defined as mixed mucinous adenocarcinoma. The nucleus is often located in the basal part of the tumor cells, and more than 90% of the tumor cells show goblet or columnar morphology, with abundant mucin in the cytoplasm^[1]. In the process of gene detection, Kirsten rat sarcoma viral oncogene (KRAS) mutation was found to be common, while epidermal growth factor receptor (EGFR) mutation was extremely rare^[2]. In the 2015 WHO classification of lung tumors, lung mucinous adenocarcinoma was divided into mucinous adenocarcinoma in situ (AIS), minimally invasive mucinous adenocarcinoma, PIMA and colloid adenocarcinoma, among which PIMA was the most common. PIMA was previously classified as mucinous

bronchoalveolar carcinoma (BAC), but other clinical and prognostic features were unclear. Pulmonary mucinous adenocarcinoma was often divided into solitary nodule or mass type and pneumonia type in CT imaging diagnosis^[3]. In this study, 78 cases of PIMA were reviewed, all patients were detected by CT examination and confirmed by pathological examination. The preoperative clinical data, laboratory examination, imaging manifestations, postoperative pathological characteristics and some gene test results were evaluated to improve the understanding, diagnosis and treatment of PIMA.

1 Materials and methods

1.1 General data

The clinical data of 78 patients with PIMA from November 2019 to November 2021 were retrospectively analyzed. All patients were received chest thin-slice CT examination and confirmed by surgery and pathology in

Anhui Provincial Chest Hospital. There were 33 males and 45 females, aged from 40 to 80 (60.3 ± 7.8) years. Inclusion criteria: All patients were received surgical treatment after evaluated by ≥ 2 thoracic surgeons according to imaging features and relevant preoperative examinations. According to the new classification criteria for pathological diagnosis jointly formulated by the International Association for the study of lung cancer, the American Thoracic Association and the European Respiratory Society in 2011 and the WHO classification in 2015, the pathological sections were judged until ≥ 2 experienced pathologists reached a consensus. The pathological diagnosis was primary PIMA, and all the pathological data were complete.

1.2 Imaging evaluation

Imaging results were obtained from the last CT scan before surgery. Imaging factors included tumor type, tumor size, nodule/mass nature (pure ground glass/ part solid/ solid), nodule/mass morphology (shallow lobulation, short fine spiculation, pleural traction, vascular convergence, smooth margin, etc.), tumor location (lobar/ peripheral/ central). The lung CT screening reporting and data system lung-RADS diagnostic grade of each nodule was determined. The C/T ratio was defined as the ratio of the maximum diameter of the solid component to the maximum diameter of the ground glass component of the pulmonary nodule. The location of the tumor was determined by the distance from each segment of the bronchus. The peripheral type was defined as a lung tumor occurring below the third-grade bronchus.

1.3 Preoperative examination and surgical management

All patients need to complete cardiopulmonary function and tumor markers examination before surgery. A few patients with a history of gastrointestinal adenocarcinoma have been pathologically diagnosed as PIMA by lung biopsy or frozen section of bronchoscopy before surgery, and secondary PIMA in the gastrointestinal tract should be excluded. Patients with suspected metastatic lesions in the nodules underwent positron emission tomography CT (PET-CT) examination. Brain magnetic resonance imaging (MRI) and whole-body bone scan were performed in patients with clinical stage Ib or above. The standard operation for radical surgery is lobectomy and ipsilateral mediastinal lymph node dissection. However, considering tumor size, C/T ratio, tumor location, potential lung function, and patient age, segmentectomy or wedge resection was performed for some nodules < 2 cm in diameter that showed ground-glass density on imaging and less than 25% solid component. Pathologic parenchymal margin was defined as the distance from the margin of the tumor to the margin of the nearest stapler confirmed by the pathologist.

1.4 Pathological evaluation

Tumor specimen surgically removed from each patient was formalin-fixed and embedded in paraffin, and the sections with the largest surface area of the tumor were measured. The microscopic hallmark of mucinous adenocarcinoma was that neoplastic cells mainly composed of goblet or columnar cells, formerly known as BAC or solid adenocarcinoma with mucinous formation, and generally considered to have an invasive component [4]. In this study, PIMA was classified according to the eighth edition of the International Lung Cancer TNM staging standard formulated by the International Association for the Study of Lung Cancer in 2017 [5]. Tumor long axis size, histological subtype, lymph node metastasis, lymphatic infiltration, vascular invasion, pleural involvement, and alveolar dissemination were evaluated. Lymph node metastasis was evaluated as positive when tumor cells were identified in the lymph nodes. Vascular invasion was evaluated as positive when tumor cells were identified in the vascular lumen. Positive pleural involvement was defined as tumor cell infiltration beyond the pleural elastic fiber layer. When tumor cells were detected in alveolar spaces, alveolar dissemination was evaluated as positive. In addition, postoperative tissue sections from a small number of patients were subjected to genetic testing and programmed cell death ligand 1 (PD-L1) expression measurement.

2 Results

2.1 Patient characteristics

The age of the patients was (60.3 ± 7.8) years, female accounted for 57.7%, non-smokers 66.7%. Ten patients (12.8%) had a family history of malignant tumors, including 4 patients with lung cancer family history. Serum carcinoembryonic antigen (CEA) was elevated ($> 5\mu\text{g/L}$) in 9 cases (11.5%). Sixty cases (76.9%) were asymptomatic and 18 cases (23.1%) had clinical symptoms. Among them, 8 cases (10.3%) had cough with mucous sputum. Because all the lesions in this study were completely resected, the preoperative clinical TNM staging was generally biased to the early stage, including 63 cases (80.8%) in stage I, 10 cases (12.8%) in stage II, and 5 cases (6.4%) in stage IIIa or above. Preoperative pulmonary function evaluation showed that all patients could tolerate surgery and were in good physical condition. The median time from screening detection to surgery was 3 months. See **Table 1**.

2.2 CT findings

Among the 78 patients, 5 cases (6.4%) were pneumonia type and 73 cases (93.6%) were nodular/mass type. The lesions were located in the left lower lobe in 27 cases (34.6%), the left upper lobe in 14 cases (17.9%), the right upper lobe in 9 cases (11.5%), the right middle lobe

in 4 cases (5.1%), and the right lower lobe in 24 cases (30.8%), including 71 cases (91.0%) of peripheral type and 7 cases (9.0%) of central type. The specific location distribution is shown in **Table 2**. The CT images of most patients showed pulmonary malignant tumor signs such as shallow lobulation, short burr, and vascular convergence sign. The CT window of 29 patients (37.2%) showed mixed ground glass density, and usually the solid component accounted for a large proportion. Forty-six cases (59.0%) showed solid nodules, of which 4 cases had smooth border and no obvious malignant tumor imaging appearance, and some cases showed cavity nodules similar to infection. Only 3 cases (3.8%) showed pure ground glass nodules in all cases. The specific lesion morphology and density characteristics are shown in **Table 2**. **Figure 1A-1D** showed the CT images of some patients.

2.3 Pathological results

According to the 2017 TNM classification, the postoperative pathological staging included 61 cases (78.2%) of stage I, 9 cases (11.5%) of stage II, and 8 cases (10.3%) of stage IIIa or above, which were

basically the same as the preoperative pathological staging. The postoperative pathological stage of 4 patients decreased compared with that before operation, which was caused by the change of tumor diameter after operation. The postoperative pathological stage of 6 patients increased compared with that before operation, including 4 cases caused by mediastinal lymph node metastasis and 2 cases caused by pleural invasion. **Table 3** showed the pathological characteristics of the patients according to the postoperative pathological report results. The median tumor diameter was 17 mm (7-85 mm). There was lymph node metastasis in 6 cases (7.7%), pleural involvement in 5 cases (6.4%), vascular invasion in 8 cases (10.3%), nerve invasion in 1 case (1.3%), bronchial margin invasion in 0 case, and interalveolar metastasis (STAS+) in 3 cases (3.8%). Thirteen patients underwent genetic testing, of whom 8 (61.5%) had KRAS mutation and 1 (7.7%) had EGFR mutation. In addition, the expression level of PD-L1 in PIMA was low. Among the 22 patients who underwent PDL-1 test, 18 patients (81.8%) had tumor proportion score (TPS) <1%, and only 2 patients (9.1%) had TPS score ≥50%. The pathological images of some PIMA patients were shown in **Figure 1E and 1F**.

Tab. 1 Clinical characteristics of 78 PIMA patients

General data	Case (%)	General data	Case (%)
Gender		Serum CEA (ng/mL)	
Male	33 (42.3)	<5.0	69 (88.5)
Female	45 (57.7)	>5.0	9 (11.5)
Age (Years)		Clinical symptoms^a	
< 60	37 (47.4)	Asymptomatic	60 (76.9)
≥60	41 (52.6)	Cough, mucus sputum	8 (10.3)
Smoking history		Chest tightness, chest and back pain	4 (5.1)
Yes	26 (33.3)	Others	6 (7.7)
No	52 (66.7)	Preoperative clinical staging	
Family history of malignant tumors		Phase I	63 (80.8)
Yes	10 (12.8)	Phase II	10 (12.8)
No	62 (79.5)	Phase IIIa and above	5 (6.4)
Unknown	6 (7.7)		

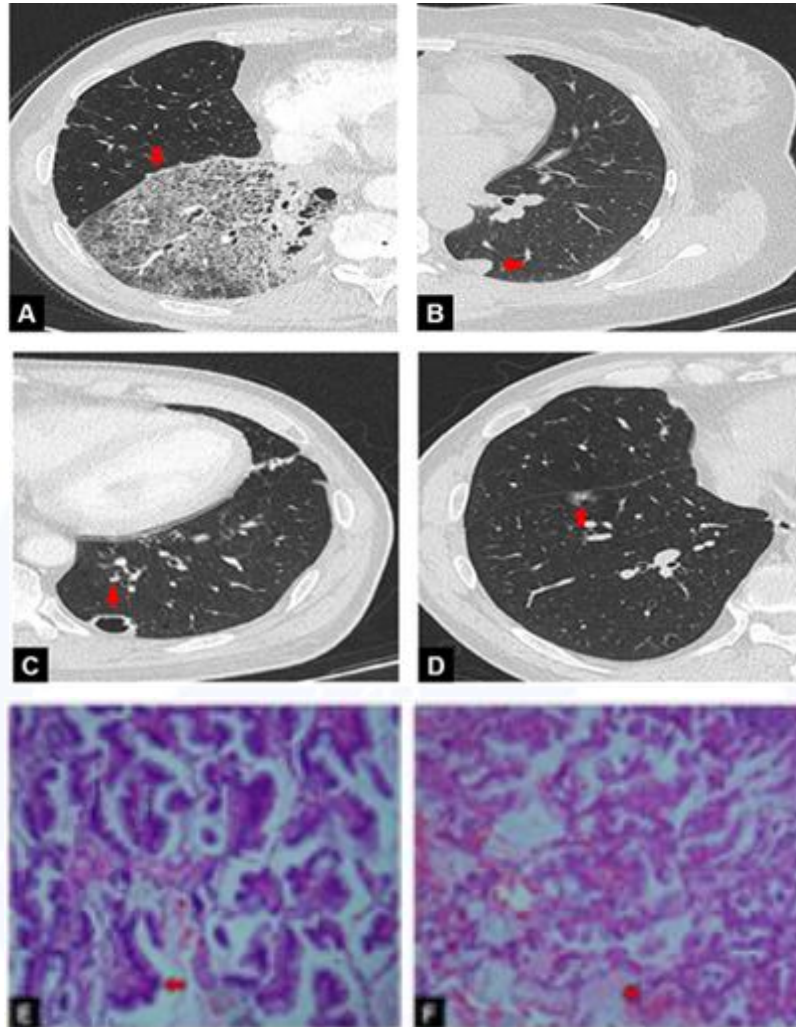
Note:^a indicates a patient may have multiple symptoms

Tab.2 Chest CT features of 78 PIMA patients

CT features	case (%)	CT features	case (%)
Type		Signs of lesions^a	
Central	7 (9.0)	Pleural traction sign	15 (19.2)
Peripheral	71 (91.0)	Short fine burr	25 (32.1)
Location		Smooth edges	4 (5.1)
Right upper lobe	9 (11.5)	Shallowly lobulated	41 (52.6)
Right middle lobe	4 (5.1)	Air bronchogram sign	29 (35.9)
Right lower lobe	24 (30.8)	Vascular convergence sign	30 (38.5)
Left upper lobe	14 (17.9)	Sign of cavity	12 (15.4)
Left lower lobe	27 (34.6)	Maximum diameter	
Type of shadow		≤3cm	62 (79.5)
Pneumonia type	5 (6.4)	>3cm- ≤5cm	9 (11.5)
Nodular/mass type	73 (93.6)	>5cm	7 (9.0)
Characteristics of nodules		Lung-RADS^b	

Solid nodule	46 (59.0)	3	5 (9.8)
Mixed ground glass nodules	29 (37.2)	4A	7 (13.7)
Pure ground glass nodules	3 (3.8)	4B	32 (62.7)
		4X	7 (13.7)

Note: ^a indicates that more than one sign may be present in one patient; ^b indicates that 51 cases were classified.



Note: A to D were CT images. A, pneumonia type, the lesion was located in the right lower lobe, showed ground glass, honeycomb-like changes, local consolidation, and cavity. B was a subpleural solid nodule in the left lower lung with regular and smooth margins. C was a cavity nodule under the pleura, and bronchial inflation is seen in part of the plane (often caused by valve obstruction after mucus enters the small airway). D was a subpleural ground glass nodule in the right lower lobar fissure, surrounded by irregular ground glass and a small number of solid components in the center. E and F showed pathological picture (HE staining, ×100), E showed a large number of columnar epithelial cells under the microscope, which were mainly adherent. F showed a large number of goblet cells with a lightly stained mucus distribution inside and outside the cytoplasm.

Fig.1 Typical CT images and pathological map of PIMA

Tab.3 Postoperative pathological characteristics of 78 PIMA patients

Pathological features	case (%)	Pathological Features	case (%)
Lymph node metastasis		Invasion and metastasis	
N0	72 (92.3)	Pleural invasion (+)	5 (6.4)
N1	3 (3.8)	Vascular invasion (+)	8 (10.3)
N2	3 (3.8)	Nerve invasion (+)	1 (1.3)
Diameter of tumor		Bronchial margin (+)	0
≤3 cm	58 (74.4)	Interalveolar metastasis (+)	3 (3.8)
>3 cm--≤5 cm	10 (12.8)	Postoperative pathological staging (TNM)	

>5 cm	10 (12.8)	Phase I	61 (78.2)
PD-L1 expression ^a		Phase II	9 (11.5)
TPS<1%	18 (81.8)	Phase IIIa and above	8 (10.3)
TPS≥1%, but<50%	2 (9.1)		
TPS≥50%	2 (9.1)		

Note: ^a indicates that 22 cases were tested.

3 Discussion

This study found that pulmonary mucinous adenocarcinoma was similar to other peripheral adenocarcinomas, female patients were slightly more than male patients, 76.9% of patients had no symptoms and were found by physical examination [6]. Most of the symptomatic patients were central type or pneumonia type, and the common symptoms were dry cough, cough mucus sputum, hemoptysis, chest tightness and chest pain. The most common symptoms were white foamy sputum and dry cough. It has been reported that pneumonia-type mucinous adenocarcinoma showed patchy density on chest CT, and may produce a large amount of foamy white sputum. In this study, chest CT showed consolidation similar to pneumonia in 5 cases, and 4 cases of them coughed foamy sputum, which may be the typical symptoms of pneumonia-type mucinous adenocarcinoma. There were 5.1% patients complained of chest tightness and chest and back pain, 11.5% patients with elevated CEA, 12.8% patients had a family history of malignant tumors, including 4 patients with a family history of lung cancer. Because all patients in this study received surgical treatment, the preoperative TNM clinical stage was relatively early, of which 80.8% were stage I, and only 6.4% were stage IIIa or above.

At present, mucinous adenocarcinoma is divided into two types according to imaging findings: pneumonia type and nodule/mass type. The prognosis of pneumonia type is usually worse [7]. Shimizu et al. [8] classified mucinous adenocarcinoma into solid or partially solid (with ground glass component) nodules without a separate classification of pneumonia type. They believed that pneumonia type mucinous adenocarcinoma did not have a special related pathogenesis, but appeared from the progression of mass type, so the pathological stage of pneumonia type was relatively late. Lee et al. [9] reported that only 23% of PIMA cases were pneumonia type, pneumonia type PIMA was more advanced in clinical and pathological stage and the prognosis was often worse than that of nodular type. All PIMA showed solid nodules or partial solid nodules, and no PIMA patients with pure ground-glass nodules were found in their study. In our study, among 78 patients with PIMA, 93.6% were solitary nodule/mass type, 6.4% were pneumonia type. The study also found that PIMA had an obvious lobar location tendency, mainly in the lower lobes of both lungs (65.4%), and the peripheral 1/3 area accounted for 91.0%, which was consistent with the study of Kim et al. [10]. In addition, 59.0% of the nodules were completely solid, followed by mixed ground glass nodules (37.2%). Most of the tumors had the imaging features of malignant tumors. The

masses were mostly shallow lobulated (41 cases), which was due to the different growth rate of the tumor to the surrounding areas. Short spiculation (25 cases) was the manifestation of cancer cells infiltrating the lung stroma. However, there are still a small number of patients with atypical imaging findings, only showing solid nodules with smooth margins or cavities with smooth margins. Therefore, these patients are easy to be misdiagnosed in clinical diagnosis, and should be paid attention to if slow growth occurs during long-term follow-up.

As a subtype of lung adenocarcinoma, PIMA is currently treated in the same way as other adenocarcinomas. Except for stage IIIB and IV, surgery is the first choice for patients with PIMA. Lobectomy plus lymph node dissection is considered the standard treatment, while sublobar resection can be used in some patients with early lung cancer or poor pulmonary function [11]. In this study, the frequency of lymph node metastasis in PIMA was low, only 7.7%, 6.4% had pleural invasion, 10.3% had vascular invasion, 1.3% had nerve invasion, and 3.8% had interalveolar metastasis. KRAS mutation was detected in 8 of 13 patients and EGFR mutation was detected in 1 patient. There were 22 patients who underwent PD-L1 detection, and 81.8% of them had TPS score <1%. According to previous reports, the mutation rate of KRAS in mucinous adenocarcinoma is 67%-92%, while that of EGFR is only 0-22% [12-13]. These results indicate that EGFR tyrosine kinase inhibitors are largely ineffective in the treatment of mucinous adenocarcinoma, and KRAS mutations may be associated with carcinogenesis of mucinous adenocarcinoma, but no relevant targeted drugs are currently available. The expression level of PD-L1 in PIMA is usually lower than that in nonmucinous adenocarcinoma, so most patients cannot be treated with immunosuppressive agents targeting PD-1/PD-L1 proteins. At present, the prognosis of PIMA is different, and some studies have shown that the overall prognosis of PIMA is worse than that of non-mucinous adenocarcinoma patients [14-15]. Xu et al. [16] showed that the overall survival of PIMA was significantly better than that of INMA in patients with the same surgical resection. Studies have found that lymph node involvement and distant organ metastasis were less common in mucinous adenocarcinoma compared with other types of non-small cell lung cancer, and dead patients usually progress to pneumonia at a later stage, and diffuse lung involvement eventually leads to respiratory failure [17].

In conclusion, this study mainly analyzed the CT findings and clinicopathological features of primary PIMA. PIMA is common in middle-aged and elderly people, and has a higher incidence in female non-smokers.

Chest CT mainly showed consolidation, which was more common in the lower lobes of both lungs, and more common in the subpleura. The proportion of solid nodules was higher, and most of them had shallow lobulation and short spiculation. Patients with elevated tumor markers had a relatively advanced stage, less pleural invasion, and a lower incidence of lymph node metastasis. The most common symptom is cough of mucinous sputum, but most patients are found by physical examination. For patients with recurrent cough with mucinous sputum, chest CT shows large patchy shadows, resembling lobar pneumonia, and no absorption of the lesions after a period of anti-infective treatment, mucinous adenocarcinoma should be considered. The KRAS mutation is more likely to occur in primary PIMA, and there is no targeted drug for this gene. The expression level of PD-L1 is low, so most patients do not respond well to immunosuppressive therapy.

There are some limitations of this study. First, all the patients were treated after 2019, and the 5-year survival rate has not been counted at present, further analysis will be conducted on the prognosis of surgical treatment for PIMA later. Secondly, it is a single-institution study with limited number of cases, and the results may be biased. In order to obtain more precise conclusions, multi-center prospective studies with larger samples should be conducted.

Conflict of Interest None

References

- [1] Chang WC, Zhang YZ, Nicholson AG. Pulmonary invasive mucinous adenocarcinoma [J/OL]. *Histopathology*, 2024, 84(1):18-31.
- [2] Gow CH, Hsieh MS, Liu YN, et al. Clinicopathological features and survival outcomes of primary pulmonary invasive mucinous adenocarcinoma[J]. *Cancers*, 2021, 13(16): 4103.
- [3] Li W, Yang Y, Yang M, et al. Clinicopathologic features and survival outcomes of primary lung mucinous adenocarcinoma based on different radiologic subtypes[J/OL]. *Ann Surg Oncol*, 2024, 31(1):167-177.
- [4] Cha YJ, Shim HS. Biology of invasive mucinous adenocarcinoma of the lung[J]. *Transl Lung Cancer Res*, 2017, 6(5): 508-512.
- [5] Chansky K, Detterbeck FC, Nicholson AG, et al. The IASLC lung cancer staging project: external validation of the revision of the TNM stage groupings in the eighth edition of the TNM classification of lung cancer[J]. *J Thorac Oncol*, 2017, 12(7): 1109-1121.
- [6] Shi XG, CAO H, TIAN CB. Clinical, CT and pathological features of pneumonic type primary pulmonary mucinous adenocarcinoma [J]. *J Clin Pulmonol*, 2020, 25(2): 271-274.
- [7] Nie K, Nie W, Zhang YX, et al. Comparing clinicopathological features and prognosis of primary pulmonary invasive mucinous adenocarcinoma based on computed tomography findings[J]. *Cancer Imaging*, 2019, 19(1): 1-8.
- [8] Shimizu K, Okita R, Saisho S, et al. Clinicopathological and immunohistochemical features of lung invasive mucinous adenocarcinoma based on computed tomography findings[J]. *Oncotargets Ther*, 2016, 10: 153-163.
- [9] Lee MA, Kang J, Lee HY, et al. Spread through air spaces (STAS) in invasive mucinous adenocarcinoma of the lung: Incidence, prognostic impact, and prediction based on clinicoradiologic factors[J]. *Thorac Cancer*, 2020, 11(11):3145-3154.
- [10] Kim DH, Bae SY, Na KJ, et al. Radiological and clinical features of screening-detected pulmonary invasive mucinous adenocarcinoma[J]. *Interact Cardiovasc Thorac Surg*, 2022, 34(2):229-235.
- [11] Yoon HJ, Kang J, Lee HY, et al. Recurrence dynamics after curative surgery in patients with invasive mucinous adenocarcinoma of the lung[J]. *Insights Imaging*, 2022, 13(1):64.
- [12] Watanabe H, Saito H, Yokose T, et al. Relation between thin-section computed tomography and clinical findings of mucinous adenocarcinoma[J]. *Ann Thorac Surg*, 2015, 99(3): 975-981.
- [13] Hata A, Katakami N, Fujita S, et al. Frequency of EGFR and KRAS mutations in Japanese patients with lung adenocarcinoma with features of the mucinous subtype of bronchioloalveolar carcinoma[J]. *J Thorac Oncol*, 2010, 5(8): 1197-1200.
- [14] Yoshizawa A, Motoi N, Riely GJ, et al. Impact of proposed IASLC/ATS/ERS classification of lung adenocarcinoma: prognostic subgroups and implications for further revision of staging based on analysis of 514 stage I cases[J]. *Mod Pathol*, 2011, 24(5): 653-664.
- [15] Russell PA, Wainer Z, Wright GM, et al. Does lung adenocarcinoma subtype predict patient survival? : a clinicopathologic study based on the new international association for the study of lung cancer/american thoracic society/european respiratory society international multidisciplinary lung adenocarcinoma classification[J]. *J Thorac Oncol*, 2011, 6(9): 1496-1504.
- [16] Xu XL, Shen WM, Wang D, et al. Clinical features and prognosis of resectable pulmonary primary invasive mucinous adenocarcinoma[J]. *Transl Lung Cancer Res*, 2022, 11(3): 420-431.
- [17] Wislez M, Antoine M, Baudrin L, et al. non-mucinous and mucinous subtypes of adenocarcinoma with bronchioloalveolar carcinoma features differ by biomarker expression and in the response to gefitinib[J]. *Lung Cancer*, 2010, 68(2): 185-191.

Submission received: 2023-09-19 / **Revised:** 2023-11-22

· 论 著 ·

肺浸润性黏液腺癌 CT 表现及临床特征分析

王保明, 代晨, 马冬春

安徽省胸科医院胸外科, 安徽 合肥 230000

摘要: 目的 探讨术后病理证实为原发性浸润性肺黏液腺癌(PIMA)患者的CT影像学表现及临床病理特征。**方法** 回顾性分析安徽省胸科医院胸外科2019年11月至2021年11月经手术后病理确诊的PIMA共78例患者的临床资料。**结果** 78例中,男33例(42.3%),女45例(57.7%),年龄(60.3±7.8)岁。血清癌胚抗原(CEA)升高(>5 ng/mL)9例(11.5%)。根据临床表现可分为无症状者60例(76.9%),有症状者18例(23.1%),包括咳嗽、咳黏液痰8例,胸闷、胸背部痛4例,其他症状6例。影像学:两肺下叶51例(65.4%)和外周型71例(91.0%),其中完全实性结节46例(59.0%),常见征象包括浅分叶、血管束束征。术后病理分期I期、II期、IIIa期及以上的患者分别为61例(78.2%)、9例(11.5%)和8例(10.3%)。13例患者行基因检测,8例检测到Kirsten大鼠肉瘤病毒癌基因(KRAS)突变,1例检测到表皮生长因子受体(EGFR)基因突变。22例患者行程序性死亡配体1(PD-L1)表达检测,其中肿瘤比例评分(TPS)<1%为18例(81.8%)。**结论** 除咳嗽为黏液痰外,PIMA临床症状无特殊;CT显示病灶发生于肺下叶和外周、完全实性多见,浅分叶、血管束束征为常见征象;实验室检测PD-L1表达水平较低;KRAS突变相对较多;这些特征在PIMA的诊断和鉴别诊断中有一定价值。

关键词: 肺黏液腺癌;肺下叶;肺外周;实性结节;浅分叶征;血管束束征;程序性死亡配体1;Kirsten大鼠肉瘤病毒癌基因;表皮生长因子受体

中图分类号: R734.2 文献标识码: A 文章编号: 1674-8182(2024)01-0052-05

CT manifestations and clinical characteristics of pulmonary invasive mucinous adenocarcinoma

WANG Baoming, DAI Chen, MA Dongchun

Department of Thoracic Surgery, Anhui Chest Hospital, Hefei, Anhui 230000, China

Corresponding author: MA Dongchun, E-mail: 1275167441@qq.com

Abstract: Objective To investigate the CT imaging manifestations and clinicopathologic features of patients with primary pulmonary invasive mucinous adenocarcinoma (PIMA) diagnosed pathologically after surgery. **Methods** The clinical data of 78 patients with PIMA diagnosed pathologically after surgery in the Department of Thoracic Surgery of Anhui Chest Hospital from November 2019 to November 2021 were retrospectively analyzed. **Results** Among the 78 cases, 33 (42.3%) were male and 45 (57.7%) were female, aged (60.3 ± 7.8) years in total, and serum carcinoembryonic antigen (CEA) was increased (> 5 ng/mL) in 9 cases (11.5%). According to the clinical characteristics, patients could be divided into the asymptomatic group (60 cases, 76.9%) and the symptomatic group (18 cases, 23.1%). The symptomatic group included 8 cases with coughing and coughing up mucus sputum, 4 cases with chest tightness and chest and back pain, and 6 cases with other symptoms. Imaging manifestations showed that 51 (65.4%) lesions were located in the inferior lobes of both lungs and 71 (91.0%) in the peripulmonary, of which 46 patients (59.0%) had completely solid nodules, and common signs included shallow lobulation and vascular cluster sign. Postoperative pathologic stages I, II, IIIa were found in 61 (78.2%), 9 (11.5%) and 8 (10.3%) patients, respectively. Moreover, genetic testing was performed in 13 patients, of which 8 cases were detected with mutations of Kirsten rat sarcoma viral oncogene (KRAS), and 1 case was detected with mutations of epidermal growth factor receptor



(EGFR) gene. Twenty-two patients were tested for the expression of programmed death-ligand 1 (PD-L1), and 18 (81.8%) of these patients had a tumor proportional score (TPS) of <1%. **Conclusion** Except for expectoration of mucous sputum, PIMA has no specific clinical symptoms. CT manifestations show that the lesions usually occur in the inferior lobes and peripulmonary of the lungs, and most pulmonary nodules are completely solid, which with signs of shallow lobulation and vascular cluster. Laboratory tests show that the expression level of PD-L1 is low, and the KRAS mutations are relatively more frequent. These features have some value in the diagnosis and differential diagnosis of PIMA.

Keywords: Pulmonary mucinous adenocarcinoma; Inferior lobe of lung; Peripulmonary; Solid pulmonary nodules; Signs of shallow lobulation; Vascular cluster sign; Programmed death-ligand 1; Kirsten rat sarcoma viral oncogene; Epidermal growth factor receptor

肺浸润性黏液腺癌 (pulmonary invasive mucinous adenocarcinoma, PIMA) 是肺腺癌的一种变异型, PIMA 的发病率低于浸润性非黏液腺癌, 占肺腺癌的 2%~5%, 可与非黏液腺癌混合存在, 对于黏液腺癌成分大于 10% 的可定义为混合型黏液腺癌, 细胞核常位于肿瘤细胞的基底部, 90% 以上的肿瘤细胞呈杯状形态或柱状形态, 胞浆内黏蛋白丰富^[1]。基因检测过程中发现其 Kirsten 大鼠肉瘤病毒癌基因 (Kirsten rat sarcoma viral oncogene, KRAS) 突变较为常见, 而表皮生长因子受体 (epidermal growth factor receptor, EGFR) 基因突变则极其少见^[2]。2015 年 WHO 对肺肿瘤分类时将肺黏液腺癌分为原位黏液腺癌、微浸润性黏液腺癌、PIMA 和胶体腺癌, 其中, PIMA 最为常见。PIMA 以前被归类为黏液性支气管肺泡癌 (BAC), 但其他临床和预后特征尚不明确。而在 CT 影像诊断上常将肺黏液腺癌分为孤立性结节或肿块型、肺炎性型^[3]。本研究报道 CT 检查发现并经病理证实的 PIMA 78 例, 评估术前临床资料、实验室检查、影像学表现、术后病理特征及部分基因检测结果等, 以提高对 PIMA 的认识及诊疗水平。

1 资料与方法

1.1 一般资料 回顾性分析 2019 年 11 月至 2021 年 11 月在安徽省胸科医院行胸部薄层 CT 检查、经手术病理证实的 PIMA 患者 78 例的临床资料。其中男 33 例, 女 45 例, 年龄 40~80 (60.3±7.8) 岁。纳入标准: 所有病例均由 ≥2 名胸外科医生根据影像学特征及相关术前检查评估为可行手术切除, 并接受手术治疗; 根据 2011 年国际肺癌研究协会、美国胸科协会、欧洲呼吸学会联合制定的病理诊断新标准分类和 2015 年 WHO 分类对病理切片做出判断, 直至 ≥2 名有经验的病理学家达成共识, 病理诊断提示原发性且为 PIMA, 且均有完整的病理资料。本研究仅分析患

者既有的临床资料, 不干扰临床诊治, 不涉及患者隐私, 符合临床研究免除伦理审查的情况。

1.2 影像学评估 依据患者术前最后一次 CT 扫描获得的影像学结果。影像学因素包括肿瘤的类型、肿瘤的大小、结节/肿块的性质 (纯磨玻璃样、部分实性、全部实性)、结节/肿块的形态 (浅分叶、短细毛刺、胸膜牵拉、血管集束、边缘光滑等)、肿瘤位置 (肺叶、周围、中央)。确定每个结节的肺 CT 筛查报告和数据库 Lung-RADS 诊断分级。C/T 比值定义为肺结节实性成分最大直径与磨玻璃成分最大直径的比值。肿瘤的位置由距离各段支气管位置确定, 周围型定义为发生于三级支气管以下的肺部肿瘤。

1.3 术前检查和手术管理 所有患者手术前均需完善心肺功能及肿瘤标志物等相关检查, 另有少数既往有胃肠道腺癌病史患者, 术前已经过肺穿刺活检或支气管镜检查的冷冻切片证实病理诊断为 PIMA, 需排除胃肠道继发性 PIMA。在对 CT 扫描结节内有可疑转移病灶的患者行正电子发射断层扫描 CT (PET-CT) 检查。对临床分期为 I b 期以上的患者进行脑磁共振成像 (MRI) 及全身骨扫描检查。根治性手术的标准术式为肺叶切除术及同侧纵隔淋巴结清扫术; 然而, 考虑到肿瘤大小、C/T 比值、肿瘤位置、潜在肺功能和患者年龄, 对部分 CT 示直径 <2 cm、磨玻璃密度且实性成分占比 <25% 的结节进行肺段切除术或楔形切除术。病理性实质切缘定义为病理科医师确认的从肿瘤边缘到最近吻合器切缘的距离。

1.4 病理学评价 每例患者手术切除的肿瘤标本经福尔马林固定, 石蜡包埋, 对肿瘤最大表面积的切片进行测量。黏液腺癌的镜下标志是肿瘤细胞, 主要由杯状或柱状细胞组成, 以前称为 BAC 或伴有黏液形成的实性腺癌, 且通常被认为具有浸润性成分^[4]。本研究将 PIMA 按照 2017 年国际肺癌研究学会制定的第八版国际肺癌 TNM 分期标准分类^[5] 确定分期。

评价肿瘤长轴大小、组织学亚型、淋巴结转移、淋巴渗透、血管浸润、胸膜受累和肺泡腔播散。在淋巴结中识别到肿瘤细胞时,将淋巴结转移评价为阳性。在血管腔中识别到肿瘤细胞时,将血管侵袭评价为阳性。当肿瘤细胞浸润超过胸膜弹力纤维层时定义为胸膜受累阳性。在肺泡腔隙中检测出肿瘤细胞时,将肺泡腔播散评价为阳性,另少部分患者的术后组织切片进行了基因检测及程序性细胞死亡配体 1 (PD-L1) 的表达水平测定。

2 结果

2.1 患者特征 女性患者(57.7%)占比稍多,其中非吸烟者 52 例(66.7%),年龄(60.3±7.8)岁。10 例(12.8%)患者有恶性肿瘤家族史,其中肺恶性肿瘤家族史 4 例。血清癌胚抗原(CEA)升高(> 5 ng/mL)9 例(11.5%)。大多数为健康体检发现的无症状者 60 例(76.9%),有临床症状者 18 例(23.1%),其中咳嗽并伴有黏液痰 8 例(10.3%)。因本研究中所有患者病灶均为手术完整切除,故术前临床 TNM 分期总体偏向于早期,其中 I 期 63 例(80.8%), II 期 10 例(12.8%), III a 期及以上 5 例(6.4%)。所有患者术前肺功能评估均可耐受手术,身体状况良好。从筛选检测到手术的中位时间为 3 个月。见表 1。

2.2 CT 表现 CT 检查结果显示,78 例患者中,肺炎型 5 例(6.4%),结节型/肿块型 73 例(93.6%);其中病灶位于左肺下叶 27 例(34.6%),左肺上叶 14 例(17.9%),右肺上叶 9 例(11.5%),右肺中叶 4 例(5.1%),右肺下叶 24 例(30.8%),其中外周型 71 例(91.0%),中央型 7 例(9.0%),具体位置分布见表 2。多数患者 CT 影像表现为浅分叶、血管束征及短毛刺等肺部恶性肿瘤征象,29 例(37.2%)患者 CT 肺窗表现为混杂磨玻璃密度,且通常实性成分占比更多。46 例(59.0%)患者表现为实性结节,其中 4 例边界光滑,无明显恶性肿瘤影像表现,另有部分患者表现为类似感染引起的空洞结节,所有病例中仅 3 例(3.8%)表现为纯磨玻璃结节,具体病灶形态与密度特征见表 2。图 1A、1B、1C、1D 为部分患者 CT 影像。

2.3 病理学结果 根据 2017 年 TNM 分类,术后病理分期中 I 期病变 61 例(78.2%), II 期病变 9 例(11.5%), III a 期病变及以上 8 例(10.3%),同术前病理分期基本一致;有 4 例患者术后病理分期较术前下降,由术后肿瘤测量直径变化引起;6 例患者术

后病理分期较术前上升,其中 4 例为纵隔淋巴结转移导致,另 2 例为胸膜侵犯导致。表 3 根据术后病理报告结果显示了患者的病理特征。肿瘤的中位直径为 17 mm(7~85 mm)。其中存在淋巴结转移 6 例(7.7%),胸膜受累 5 例(6.4%),脉管侵犯 8 例(10.3%),神经侵犯 1 例(1.3%),支气管切缘侵犯 0 例,肺泡间转移(STAS+)患者 3 例(3.8%)。13 例患者进行了基因检测,其中 8 例(61.5%)存在 KRAS 突变,1 例(7.7%)存在 EGFR 突变。此外,PIMA 表达 PD-L1 水平较低,22 例患者进行了 PDL-1 检测,其中肿瘤比例评分(tumor proportion score, TPS)<1%共 18 例(81.8%),而 TPS 评分≥50%仅 2 例(9.1%)。部分 PIMA 患者病理图见图 1E、1F。

表 1 78 例 PIMA 患者临床特征
Tab. 1 Clinical characteristics of 78 PIMA patients

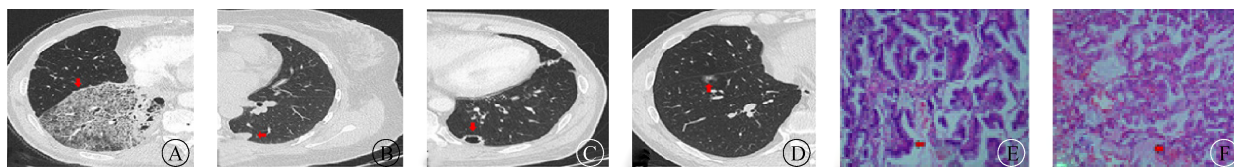
基本资料	例(%)	基本资料	例(%)
性别		血清 CEA(ng/mL)	
男	33(42.3)	<5.0	69(88.5)
女	45(57.7)	≥5.0	9(11.5)
年龄(岁)		临床症状 ^a	
<60	37(47.4)	无症状	60(76.9)
≥60	41(52.6)	咳嗽、咳黏液痰	8(10.3)
吸烟史		胸闷、胸背部痛	4(5.1)
是	26(33.3)	其他	6(7.7)
否	52(66.7)	术前临床分期	
恶性肿瘤家族史		I 期	63(80.8)
有	10(12.8)	II 期	10(12.8)
无	62(79.5)	III a 期及以上	5(6.4)
不详	6(7.7)		

注:^a表示一例患者可有多个症状。

表 2 78 例 PIMA 患者胸部 CT 特征
Tab. 2 Chest CT features of 78 PIMA patients

胸部 CT 特征	例(%)	胸部 CT 特征	例(%)
类型		病灶征象 ^a	
中央型	7(9.0)	胸膜牵拉征	15(19.2)
周围型	71(91.0)	短细毛刺	25(32.1)
位置		边缘光滑	4(5.1)
右上肺叶	9(11.5)	浅分叶状	41(52.6)
右中肺叶	4(5.1)	支气管充气征	29(35.9)
右下肺叶	24(30.8)	血管束束征	30(38.5)
左上肺叶	14(17.9)	空洞征	12(15.4)
左下肺叶	27(34.6)	最大直径	
阴影分型		≤3 cm	62(79.5)
肺炎型	5(6.4)	>3 cm 但≤5 cm	9(11.5)
结节型/肿块型	73(93.6)	>5 cm	7(9.0)
结节特征		Lung-RADS 分类 ^b	
实性结节	46(59.0)	3	5(9.8)
混杂磨玻璃结节	29(37.2)	4A	7(13.7)
纯磨玻璃结节	3(3.8)	4B	32(62.7)
		4X	7(13.7)

注:^a表示一例患者可存在多个征象;^b表示做了 51 例分类。



注:A~D为CT影像,A为肺炎型,病灶位于右下肺叶,呈磨玻璃、蜂窝状改变,局部实变,内见空洞;B为左下肺胸膜下实性结节,边缘规则、光滑;C为胸膜下的空洞结节,部分层面见支气管充气(黏液进入小气道后常引起活瓣性阻塞所致);D为右下肺叶间裂胸膜下磨玻璃结节,周围不规则磨玻璃,中央少量实性成分;E、F为病理图(HE染色,×100),E为显微镜下见大量柱状上皮细胞,贴壁生长为主;F为见大量杯状细胞,细胞浆内外见淡染的黏液分布。

图1 PLMA的典型CT影像和病理图

Fig. 1 Typical CT images and pathological map of PIMA

表3 78例患者PIMA术后病理特征
Tab. 3 Postoperative pathological characteristics of 78 PIMA patients

病理特征	例(%)	病理特征	例(%)
淋巴结转移		浸润与转移	
N0	72 (92.3)	胸膜侵犯(+)	5 (6.4)
N1	3 (3.8)	脉管侵犯(+)	8 (10.3)
N2	3 (3.8)	神经侵犯(+)	1 (1.3)
肿瘤直径		支气管切缘(+)	0
≤3 cm	58 (74.4)	肺泡间转移(+)	3 (3.8)
>3 ~ ≤5 cm	10 (12.8)	术后病理分期(TNM)	
>5 cm	10 (12.8)	I期	61 (78.2)
PD-L1 表达水平 ^a		II期	9 (11.5)
TPS评分<1%	18 (81.8)	IIIa期及以上	8 (10.3)
TPS评分≥1%~<50%	2 (9.1)		
TPS≥50%	2 (9.1)		

注:^a表示检测了22例。

3 讨论

本研究发现肺黏液腺癌与其他周围型腺癌相似^[6],女性患者稍多于男性,76.9%患者无任何症状,仅由健康体检发现,有症状者多为中央型或肺炎型患者,常见症状主要是干咳、咳黏液痰、咯血、胸闷及胸痛等。最常见症状为咳白色泡沫样痰、干咳。有文献显示肺炎型黏液性腺癌胸部CT显示片状密度增高影,可咳大量泡沫样白痰^[7]。本研究5例胸部CT呈现类似于肺炎的实变影,其中4例咳泡沫样痰,此症状可能为肺炎型黏液腺癌的典型症状。以胸闷、胸背部疼痛为主诉的患者5.1%。11.5%出现CEA升高。12.8%有恶性肿瘤家族史,其中4例有肺恶性肿瘤家族史。因本研究中所有患者均接受外科手术,故术前TNM临床分期多数为早期,其中I期占80.8%,IIIa期及以上仅占6.4%。

目前黏液腺癌依据影像学表现分为肺炎型和结节型/肿块型两种类型,肺炎型的预后通常更差^[7]。Shimizu等^[8]研究将黏液腺癌分为实性或部分实性(伴磨玻璃成分)结节,而无单独分类的肺炎型,其认为肺炎型并无特殊的相关发病机制,而是由肿块型进

展而出现,因此肺炎型的病理分期相对更晚。Lee等^[9]报告的PIMA病例中肺炎型仅占23%,进一步指出肺炎型PIMA在临床和病理学上偏晚期,预后往往比结节型差,且所有PIMA均表现为实性结节或部分实性结节,其研究中未发现CT表现为纯磨玻璃样结节的PIMA患者。本研究78例PIMA患者中,孤立结节型/肿块型共93.6%,肺炎型仅6.4%。本研究还发现,PIMA有明显的肺叶位置倾向,以两肺下叶为主(65.4%),且外周1/3区占91.0%,与Kim等^[10]研究结果一致。此外,59.0%为完全实性结节,其次为混杂磨玻璃结节(37.2%);大多数存在恶性肿瘤的影像学表现,肿块多表现为浅分叶(41例),是由于肿瘤向四周的生长速度不同所致;血管集束征(30例)反映病灶组织供血比较丰富,利于病灶组织的生长;短毛刺(25例)是癌细胞浸润肺间质的表现。但仍有少部分患者影像学表现极不典型,仅表现为边缘光滑的实性结节或空洞结节,在临床诊断中极易误诊,如长期随访复查出现缓慢增长时,需引起重视。

PIMA作为肺腺癌的一种亚型,目前主要治疗方式与其他腺癌相同,除IIIb期和IV期外,手术是PIMA患者的首选治疗方法。肺叶切除加淋巴结清扫术被认为是标准治疗方法,而亚肺叶切除可用于部分早期肺癌或肺功能低下的患者^[11]。本研究中,PIMA的淋巴结转移率较低,仅7.7%,6.4%有胸膜侵犯,10.3%脉管侵犯,1.3%神经侵犯,3.8%肺泡间转移。有13例患者行基因检测,8例检测到KRAS突变,1例EGFR突变。22例患者行PD-L1检测,TPS评分<1%共81.8%。根据既往报告,黏液腺癌中KRAS突变率为67%~92%,而EGFR仅为0~22%^[12-13]。以上结果表明,EGFR酪氨酸激酶抑制剂对黏液腺癌治疗基本无效,KRAS突变可能与黏液腺癌的癌变相关,但目前尚无相关靶向药物上市。PIMA的PD-L1表达水平通常低于非黏液腺癌,因此多数患者无法使用针对PD-1/PD-L1蛋白的免疫抑制剂治疗。目前关于

PIMA的预后说法不一,有研究显示,其总体预后比非黏液腺癌差^[14-15]。Xu等^[16]研究显示,同样经手术切除,肺IMA患者的总生存期显著优于肺非浸润性黏液腺癌。有研究发现黏液腺癌与其他类型的非小细胞肺癌相比,其淋巴结受累和远处脏器转移更少,死亡患者通常是后期进展至肺炎型,肺部弥漫性受累最终导致呼吸衰竭^[17]。

综上所述,本研究主要分析了原发性PIMA的CT表现及临床病理特征,其常见于中老年人,女性非吸烟者发病率更高。胸部CT以实变影为主,好发于双肺下叶,胸膜下多见,实性结节比例更高,多数有浅分叶、血管集束征等肺恶性肿瘤表现。肿瘤标记物升高的患者分期相对较晚,胸膜受侵犯较少见,淋巴结转移发生率低。常见症状为咳黏液痰,但多数患者由体检发现,对于反复咳嗽伴黏液痰,胸部CT提示较大片状影,似大叶性肺炎,经一段时间抗感染治疗病灶未见吸收者,需考虑黏液腺癌的可能。KRAS突变在原发性PIMA中出现几率较高,暂无针对该基因的靶向药物;PD-L1表达水平较低,因此多数患者免疫抑制治疗效果欠佳。

本研究存在一些局限性,首先,所有患者均为2019年后就治疗,尚未统计术后5年生存率,后期将进一步分析手术治疗PIMA的评价及预后。其次,是病例数量有限的单机构研究,结果可能存在偏差;为获得更精确的结论,应进行多中心、更大样本的前瞻性研究。

利益冲突 无

参考文献

- [1] Chang WC, Zhang YZ, Nicholson AG. Pulmonary invasive mucinous adenocarcinoma [J/OL]. *Histopathology* (2023-10-22) [2023-11-22]. <https://pubmed.ncbi.nlm.nih.gov/37867404/>.
- [2] Gow CH, Hsieh MS, Liu YN, et al. Clinicopathological features and survival outcomes of primary pulmonary invasive mucinous adenocarcinoma [J]. *Cancers*, 2021, 13(16): 4103.
- [3] Li W, Yang Y, Yang M, et al. Clinicopathologic features and survival outcomes of primary lung mucinous adenocarcinoma based on different radiologic subtypes [J/OL]. *Ann Surg Oncol* (2023-11-05) [2023-11-22]. <https://pubmed.ncbi.nlm.nih.gov/37925652/>.
- [4] Cha YJ, Shim HS. Biology of invasive mucinous adenocarcinoma of the lung [J]. *Transl Lung Cancer Res*, 2017, 6(5): 508-512.
- [5] Chansky K, Detterbeck FC, Nicholson AG, et al. The IASLC lung cancer staging project: external validation of the revision of the TNM stage groupings in the eighth edition of the TNM classification of lung cancer [J]. *J Thorac Oncol*, 2017, 12(7): 1109-1121.
- [6] 陈武,宋彪,王彬,等.原发性肺黏液腺癌的CT影像诊断[J].*中华全科医学*,2023,21(7):1197-1201.
Chen W, Song B, Wang B, et al. CT imaging diagnosis of primary pulmonary mucinous adenocarcinoma [J]. *Chinese Journal of General Practice*, 2023, 21(7): 1197-1201.
- [7] Nie K, Nie W, Zhang YX, et al. Comparing clinicopathological features and prognosis of primary pulmonary invasive mucinous adenocarcinoma based on computed tomography findings [J]. *Cancer Imaging*, 2019, 19(1): 47.
- [8] Shimizu K, Okita R, Saisho S, et al. Clinicopathological and immunohistochemical features of lung invasive mucinous adenocarcinoma based on computed tomography findings [J]. *Oncol Targets Ther*, 2016, 10: 153-163.
- [9] Lee MA, Kang J, Lee HY, et al. Spread through air spaces (STAS) in invasive mucinous adenocarcinoma of the lung: Incidence, prognostic impact, and prediction based on clinicoradiologic factors [J]. *Thorac Cancer*, 2020, 11(11): 3145-3154.
- [10] Kim DH, Bae SY, Na KJ, et al. Radiological and clinical features of screening-detected pulmonary invasive mucinous adenocarcinoma [J]. *Interact Cardiovasc Thorac Surg*, 2022, 34(2): 229-235.
- [11] Yoon HJ, Kang J, Lee HY, et al. Recurrence dynamics after curative surgery in patients with invasive mucinous adenocarcinoma of the lung [J]. *Insights Imaging*, 2022, 13(1): 64.
- [12] Watanabe H, Saito H, Yokose T, et al. Relation between thin-section computed tomography and clinical findings of mucinous adenocarcinoma [J]. *Ann Thorac Surg*, 2015, 99(3): 975-981.
- [13] Hata A, Katakami N, Fujita S, et al. Frequency of EGFR and KRAS mutations in Japanese patients with lung adenocarcinoma with features of the mucinous subtype of bronchioloalveolar carcinoma [J]. *J Thorac Oncol*, 2010, 5(8): 1197-1200.
- [14] Yoshizawa A, Motoi N, Riely GJ, et al. Impact of proposed IASLC/ATS/ERS classification of lung adenocarcinoma: prognostic subgroups and implications for further revision of staging based on analysis of 514 stage I cases [J]. *Mod Pathol*, 2011, 24(5): 653.
- [15] Russell PA, Wainer Z, Wright GM, et al. Does lung adenocarcinoma subtype predict patient survival? : a clinicopathologic study based on the new international association for the study of lung cancer/american thoracic society/european respiratory society international multidisciplinary lung adenocarcinoma classification [J]. *J Thorac Oncol*, 2011, 6(9): 1496-1504.
- [16] Xu XL, Shen WM, Wang D, et al. Clinical features and prognosis of resectable pulmonary primary invasive mucinous adenocarcinoma [J]. *Transl Lung Cancer Res*, 2022, 11(3): 420-431.
- [17] Wislez M, Antoine M, Baudrin L, et al. Non-mucinous and mucinous subtypes of adenocarcinoma with bronchioloalveolar carcinoma features differ by biomarker expression and in the response to gefitinib [J]. *Lung Cancer*, 2010, 68(2): 185-191.

收稿日期:2023-09-19 修回日期:2023-11-22 编辑:王国品